Evidence for Collisional Damping in High-Energy Raman-Scattering Experiments at 0.26 μm

R. E. Turner, Kent Estabrook, R. L. Kauffman, D. R. Bach,[a] R. P. Drake, D. W. Phillion, B. F. Lasinski, E. M. Campbell, W. L. Kruer, and E. A. Williams
Lawrence Livermore National Laboratory, University of California, Livermore, California 94550
(Received 28 August 1984)

Experiments using 1.5 kJ of 0.26-μm wavelength light to irradiate thin "burn-through" targets show less stimulated Raman scattering (SRS) than similar experiments at 0.53 μm. The SRS from high-Z (Au) targets is 3 orders of magnitude less than SRS from low-Z (CH) targets irradiated at similar intensities. These results are the first direct observation of collisional damping of the Raman instability in high-Z targets as predicted by theory and simulations.

PACS numbers: 52.50.Jm, 52.25.Rv, 52.35.Py, 52.40.Db

Raman scattering[1-5] (SRS) in laser-produced plasmas can generate high-energy electrons, which can degrade laser-fusion target gain. In nearly all previous laser-plasma experiments, SRS has been limited by steep density gradients, which restrict the phase-matching regions to relatively small lengths. However, the reactor-size targets envisioned for future laser-fusion experiments will produce much longer density-gradient lengths. Here we report the observation of an important alternative limiting mechanism, electron-ion collisions, which can inhibit SRS.

In these experiments, uv laser light irradiates thin films causing them to expand rapidly. By the peak of the 1-nsec laser pulse, the electron density is near resonance ($n_c/4$) for the Raman[5] and $2\omega_{pe}$ [6] instabilities. Other instabilities that can produce hot electrons occur near critical density $\{n_c = 10^{21}[(1.06\ \mu\text{m})/\lambda_0]^2\ e^-/\text{cm}^3\}$ and are thus mostly excluded from these observations. With plastic (CH) targets, the fraction of the incident energy scattered as Raman light is 5 times smaller for irradiations with a laser wavelength (λ_0) of 0.26 μm than for 0.53 μm. With Au targets, the decrease is more than 4 orders of magnitude. We use theory and simulations to show that the suppression of SRS with increasing laser frequency or target Z is due to collisional damping of SRS.

These experiments used one arm of the 74-cm-aperture Novette laser.[7] An array of potassium dihydrogen phosphate crystals quadrupled the frequency of the 1.05-μm laser light to produce up to 1.5 kJ of light at 0.26-μm wavelength in a near Gaussian pulse of 0.9–1.2 nsec full width at half maximum (FWHM).[8] A mask at the center of the lens and the chromatic aberration of the $f/4$ focusing lens caused the uv light to focus in a region free from residual 1.05-μm and 0.53-μm light.[7] The experimental intensities quoted here are the average laser power divided by the illuminated area as determined from x-ray micrographs (x-ray energy of $\sim$ 1–1.5 keV). We define the beam diameter, D, as the FWHM of the x-ray intensity. Although the laser beam is known to be nonuniform,[9] and qualitatively less uniform than the beam at 0.53 μm, localized regions of higher intensities should enhance, not reduce, the growth of Raman scattering.

The targets were 6-μm-thick CH or 0.4-μm-thick Au foils, supported on large washers. The thicknesses were chosen, by LASNEX calculations, so that the maximum electron density on-axis would be slightly less than $n_c/4$ by the peak of the laser pulse. The parabolic density scale lengths[1] are calculated to be (500–1000)λ_0 in both the axial and radial directions for both CH and Au. The targets were irradiated at normal incidence, with the focus in front of the target. The focal-spot diameters were 300 to 350 μm, resulting in average target-plane intensities of $(1-2)\times 10^{15}$ W/cm^2.

A streak camera and optical system, mounted orthogonal to the laser beam, provided time-resolved one-dimensional spatial images along the direction of the laser axis.[10] This instrument looked at the 313-nm bremsstrahlung emission from both the front and the back expanding plasmas. When the plasma is optically thin (low-Z green experiments), this emission is proportional to the line-averaged product of the density squared and the square root of the temperature. The simulation line integrals are in good agreement. A time-resolved optical spectrometer measured the Raman light scattered at 135° to the laser beam. Calibrated photodiodes, filtered to look only at SRS from below $n_c/4$ ($0.35\ \mu\text{m} < \lambda_0 < 0.5\ \mu\text{m}$), measured the absolute level of Raman-scattered light at various angles (between 105° and 169° from the laser). Spectroscopy verified that all Raman light emissions were within this range of wavelengths.

The results are summarized in Fig. 1. The error bars enclose all the data obtained during the experiments. We estimate the absolute accuracy to be within a factor of 2; the principal source of error arises from the finite number (10) of photodiodes and the resulting uncertainty in the true angular distribition of the scattered light. The data analysis is identical to that discussed by Drake *et al.*[11] Most of the SRS energy was within 45° of direct backscatter, although no measurements were made back through the $f/4$ lens.

Figure 1 also shows the data from previous 0.53-μm

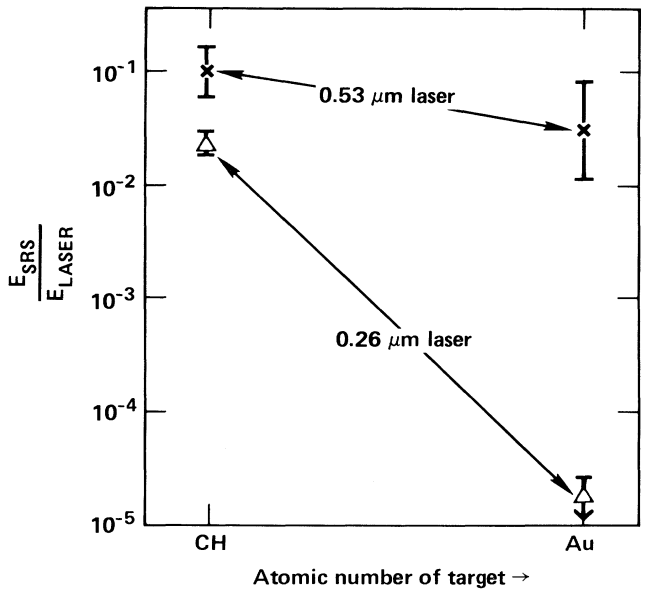

FIG. 1. Energy in Raman-scattered light from low-Z and high-Z thin-foil targets. All cases have intensities $\sim 10^{15}$ W/cm^2. The gold data point for 0.26 μm is an upper limit.

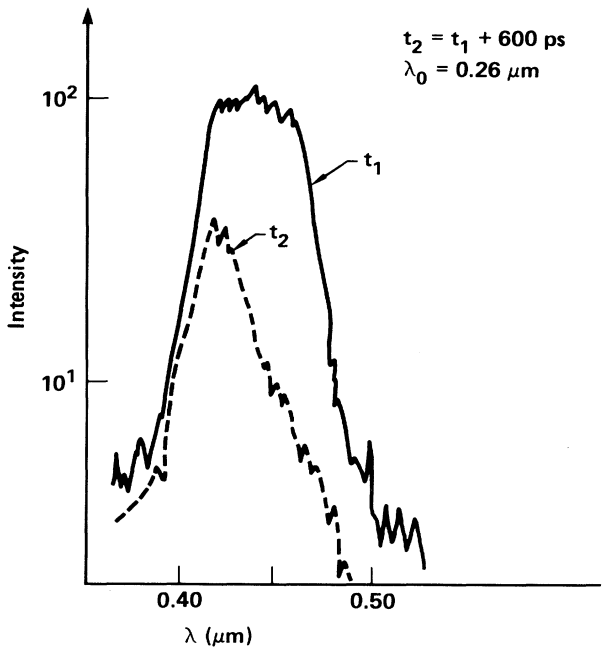

FIG. 2. Stimulated Raman-scattering spectrum from a CH (plastic) target. t_1 is the peak time of the SRS pulse.

experiments[11] conducted at similar average intensities and D/λ_0, where λ_0 is the incident wavelength. The foils were thinner, to allow the density to drop below $n_c/4$ for the 0.53-μm light before the peak of the laser pulse. These green-light experiments produced very large amounts of SRS. Note that at these intensities ($\gtrsim 10^{15}$), the Z dependence in the level of Raman scattering is small for the 0.53-μm experiments. In contrast, for the 0.26-μm experiments, Raman scattering decreases greatly with the increase in atomic number. For the CH targets, the energy in Raman-scattered light is approximately 2% of the incident laser energy. For the gold targets, any SRS light present was below the minimum detectability of the diodes, setting an upper limit for the energy of $\sim 10^{-5}$ of the laser energy. We attribute this dramatic change to collisional damping, as discussed below.

Figure 2 shows the Raman light spectrum from a CH target, at two different times in the laser pulse. This spectral shape is remarkably similar, when scaled by the wavelength ratio, to the data obtained during the 0.53-μm thin-foil experiments.[11] The wavelength of the SRS implies that the scattering is taking place at densities between $0.1n_c$ and $0.2n_c$. Assuming that the shortest-wavelength Raman light is limited by Landau damping of the corresponding plasma wave, we estimate the electron temperature to be ~ 2 keV. The decrease in the longest-wavelength Raman light at later times is due to the decreasing plasma density.

To clearly identify collisional effects, an experiment must exceed the competing gradient-scale-length threshold. Figure 3 is a contour plot from a LASNEX[12] two-dimensional (2D) hydrodynamic simulation of a CH foil showing the large region of relatively constant density plasma. The hydrodynamic calculations are consistent with several (indirect) density measure-

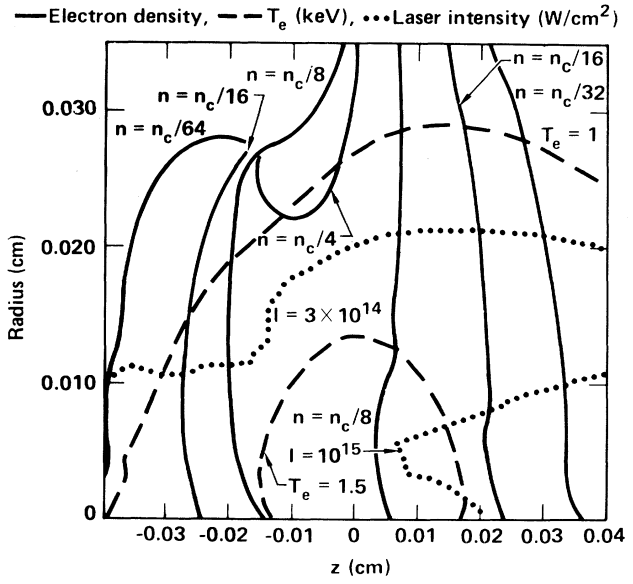

FIG. 3. Contour plots of density, temperature, and laser intensity from a 2D simulation (LASNEX) at a time 200 psec before the laser pulse peak intensity. $\lambda_0 = 0.26$ μm, 6-μm-thick CH, 1400 J, spot diameter = 385 μm.

ments: the time- and spatially-resolved bremsstrahlung[10] and the time-resolved SRS spectrum. They were further verified in the 0.53-μm experiments,[11] by the timing of the emitted ($\frac{3}{2}$) harmonic of the incident light and the timing of the burn-through of the laser light. The SRS is above the density-scale-length threshold, which is of order 4×10^{13} W/cm^2 from Eq. (7) of Ref. 1 for a parabolic density profile. Plasma turbulence, Brillouin sidescattering and backscattering, and light filamentation can change the thresholds although these effects are difficult to quantify. Time-integrated x-ray microscope pictures at 45°, 75°, and 135° from the laser beam show no structures which could be interpreted as filaments. The theoretical and computational studies reported in this Letter and by Estabrook, Kruer, and Baily[13] indicate that thermal filamentation is stabilized here. The diverging laser beam contributes to the stability.[13]

Electron-ion collisions reduce SRS by (1) directly damping the electron plasma waves, (2) absorbing the scattered light wave that amplifies Raman scattering, and (3) absorbing the incident laser light directly. The collisional threshold[5] in a plasma of constant electron density n is

$$\gamma^2 > (\nu_{ei}/2)(\omega_p/\omega_s)^2[(\nu_{ei}/2)+\omega_i], \tag{1}$$

where ω_i is the electron Landau damping rate and ν_{ei} is the electron-ion collision frequency[14] relevant to high-frequency waves. ν_{ei} is $\approx 9\times10^{-11}\bar{z}n\ln\Lambda T_e^{-3/2}$ sec^{-1}, where $\ln\Lambda\approx 31-\ln(n^{1/2}/T_e)$, $\bar{z}$ is the average ionization state, T_e is in kiloelectronvolts, and n is in inverse cubic centimeters.

The Raman backscattering growth rate[4] is

$$\gamma \sim (k_{\rm epw}/4)v_{\rm osc}[(\omega_p/\omega_s)(\omega_p/\omega_{\rm epw})]^{1/2}[1-(n/n_c)]^{-1/4}\ \text{sec}^{-1}, \tag{2}$$

where ω_s, ω_p, and $\omega_{\rm epw}$ are the scattered, plasma, and electron plasma wave frequencies, respectively. Here $k_{\rm epw}$ is the wave vector of the electron plasma wave

$$\sim \omega_0/c\,\{[1-(n/n_c)]^{1/2}+[1-2(n/n_c)^{1/2}]^{1/2}\}$$

for $k\lambda_D << 1$, and

$$v_{\rm osc} = \{I(\text{W/cm}^2)[\lambda_0/(1.06\ \mu\text{m})]^2/1.2\times10^{18}\}^{1/2}c.$$

Equations (1) and (2) determine a collisional threshold intensity:

$$I > 3\times10^{-12}(k_{\rm epw}c/\omega_0)^{-2}(\omega_{\rm epw}/\omega_s)\nu_{ei}[(\nu_{ei}/2)+\omega_i]\ \text{W/cm}^2\propto\lambda_0^{-3}. \tag{3}$$

(The wavelength scaling is from the analysis below.)

Kinetic simulations[5] of Raman backscattering with collisions show that SRS at $n/n_c\sim0.2$ is severely reduced for $\nu_{ei}/\gamma\sim0.6$–0.8, a somewhat lower value than the collisional threshold condition of $\nu_{ei}/\gamma\sim2$ from Eq. (1).

To calculate ν_{ei}, one must know T_e and $\bar{z}$. We estimated the electron temperature of CH targets using the short-wavelength cutoff of the SRS spectra and using time-resolved x-ray spectroscopic data[11] from CH targets doped with a small amount of sulfur. Both of these measurements give $T_e\approx2$ keV. Two-dimensional LASNEX calculations for gold (similar to Fig. 3) show $T_e\sim3$ keV and $\bar{z}\sim56$. Note from Fig. 3 that inverse bremsstrahlung absorption reduced the incident laser intensity a factor of 2–3 before reaching the density where most of the Raman scattering occurred (similarly for the Au target). Table I shows estimates for ν_{ei}/γ for $\lambda_0=0.26$-μm and $\lambda_0=0.53$-μm (Ref. 11) experiments. Note that for the 0.26-μm cases, $\nu_{ei}/\gamma\approx1$ for Au; for CH, with $\bar{z}$ a factor of ~15 smaller, $\nu_{ei}/\gamma << 1$. This can account for the large difference in the observed SRS.

Finally, we use LASNEX simulations[15] of thick gold disks to roughly estimate the scaling of ν_{ei}/γ. Least-squares fits of T_e and $\bar{z}$ from 1-nsec, 450-μm laser-spot-diameter runs are

$$T_e\sim1.2\times10^{-6}I^{0.45}[\lambda_0/(1.06\ \mu\text{m})]^{0.85}$$

and

$$\bar{z}\sim4.8I^{0.067}[\lambda_0/(1.06\ \mu\text{m})]^{-0.06}.$$

These T_e and $\bar{z}$ are consistent with the thin-film results (Fig. 3). T_e and $\bar{z}$ also increase with the spot size and pulse length and are sensitive to other geometric factors. We use a heat-flux limit $f=0.03$ for $\lambda_0\gtrsim0.53$

TABLE I. Ratio of collision frequency to growth rate and experimental results.

λ_0 (μm)	Target	ν_{ei}/γ_0	Raman yield ($E_{\rm SRS}/E_{\rm laser}$)
0.26	CH	0.2	0.02
0.26	Au	1.8	$<10^{-5}$
0.53	CH	0.04	0.10
0.53	Au	0.2	0.04

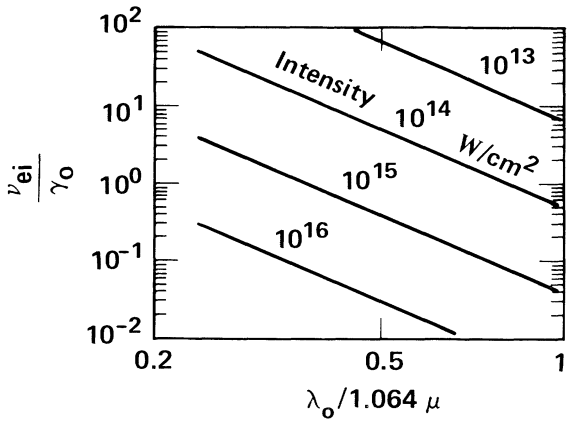

FIG. 4. Rough scaling of (collision frequency)/(Raman growth rate) (ν_{ei}/γ) vs laser wavelength for a variety of laser intensities on gold disks; ν_{ei} is calculated for $n = n_c/4$.

μm and $f = 0.1$ for $\lambda_0 = 0.26$. Solving for ν_{ei}/γ from these fits and Eq. (2) gives

$$\frac{\nu_{ei}}{\gamma} \sim 0.04\left(\frac{I}{10^{15}\ \mathrm{W/cm^2}}\right)^{-1.1}\left(\frac{\lambda_0}{1.06\ \mu\mathrm{m}}\right)^{-3.3}$$

which is plotted in Fig. 4.

In summary, we have presented experimental data showing reduced Raman scattering from low-Z targets irradiated with 0.26-μm laser light, compared to those irradiated with 0.53-μm light. Raman scattering was not observed from large-scale-length high-Z plasmas similarly irradiated with 0.26-μm light. These results are consistent with calculations and simulations, which indicate that the suppression of SRS is due to collisions.

We acknowledge the considerable efforts of the laser operations and the target fabrication groups and the support of John Emmett. This work was performed under the auspices of the U. S. Department of Energy by the Lawrence Livermore National Laboratory under Contract No. W7405-ENG-48.

---

[a]Permanent address: Los Alamos National Laboratory, Los Alamos, N. Mex. 87545.

[1]H. Figueroa *et al.*, Phys. Fluids **27**, 1887 (1984).

[2]W. C. Mead *et al.*, Phys. Fluids **26**, 2316 (1983).

[3]K. Tanaka *et al.*, Phys. Rev. Lett. **48**, 1179 (1982); C. C. Shepard *et al.*, Bull. Am. Phys. Soc. **28**, 1058 (1983); D. Phillion *et al.*, Phys. Fluids **25**, 1434 (1982), and Phys. Rev. Lett. **49**, 1405 (1982); see also A. A. Offenberger *et al.*, Phys. Rev. Lett. **49**, 371 (1982); R. G. Watt *et al.*, Phys. Rev. Lett. **41**, 170 (1978); R. G. Watt and Z. A. Pietrzyk, Appl. Phys. Lett. **37**, 1068 (1980).

[4]C. S. Liu *et al.*, Phys. Fluids **17**, 1211 (1974); J. F. Drake *et al.*, Phys. Fluids **17**, 778 (1984); D. W. Forslund, J. M. Kindel, and E. L. Lindman, Phys. Fluids **18**, 1002 (1975).

[5]Kent Estabrook and W. L. Kruer, Phys. Rev. Lett. **53**, 465 (1984), and references within.

[6]A. B. Langdon *et al.*, Phys. Rev. Lett. **43**, 133 (1979).

[7]Lawrence Livermore National Laboratory 1982 Laser Program Annual Report, 1983 (unpublished), Sec. 2.

[8]K. R. Manes *et al.*, in Proceedings of the Conference on Lasers and Electroptics, Los Angeles, 1984 (to be published), paper No. TUB37.

[9]K. R. Manes and W. W. Simmons, Lawrence Livermore National Laboratory Report No. UCRL-90158 (to be published).

[10]D. W. Phillion *et al.*, to be published.

[11]R. P. Drake *et al.*, Phys. Rev. Lett. **53**, 1739 (1984), and to be published.

[12]G. B. Zimmerman and W. L. Kruer, Comments Plasma Phys. Controlled Fusion **2**, 51 (1975).

[13]K. Estabrook, W. L. Kruer, and D. S. Bailey, to be published.

[14]A. B. Langdon, Phys. Rev. Lett. **44**, 575 (1980).

[15]K. Estabrook *et al.*, Phys. Rev. Lett. **46**, 724 (1981); M. D. Rosen, private communication.